# Colloidal Plasmonic DNA-Origami with Photo-Switchable Chirality in Liquid Crystals

QINGKUN LIU,[1] ANTON KUZYK,[2] MASAYUKI ENDO,[3] IVAN SMALYUKH[1,4,5,*]

[1]*Department of Physics, University of Colorado, Boulder, CO 80309, USA*
[2]*Department of Neuroscience and Biomedical Engineering, Aalto University School of Science, P.O. Box 12200, FI-00076 Aalto, Finland*
[3]*Department of Chemistry, Graduate School of Science,Kyoto University, Yoshida-ushinomiyacho, Sakyo-ku, Kyoto 606-8501, Japan*
[4]*Department of Electrical, Computer, and Energy Engineering, Materials Science and Engineering Program and Soft Materials Research Center, University of Colorado, Boulder, CO 80309, USA*
[5]*Renewable and Sustainable Energy Institute, National Renewable Energy Laboratory and University of Colorado, Boulder, CO 80309, USA*
**Corresponding author: ivan.smalyukh@colorado.edu*

**Photo-responsive nanomaterials hold great promise for realizing information processing devices, micro-machines and biosensors. Scalable assembly of such materials using mesostructured liquids such as liquid crystals remains a challenge due to the poor compatibility of nanostructures and the host medium. Here we demonstrate a new type of colloidal dispersion of plasmonic DNA-origami with photo-switchable chirality in cellulose nanofiber-based liquid crystals. The composite material inherits properties of DNA-origami plasmonic nanostructures, so that the composite's chirality can be erased by ultraviolet light and recovered by visible light. The cellulose nanofibers provide a liquid crystalline host with weak optical birefringence, which barely affects the polarization of the incident light, so that the response is dominated by circular dichroism of uniformly dispersed plasmonic nanostructures. Our approach may serve as a new platform for scalable assembling DNA origami-templated nanomaterials.** 

Photo active materials exhibit remarkable functional properties for information storage, nano-machines and biological applications [1-3]. Several techniques have been developed to fabricate such photo-responsive materials, including molecular motors [4,5] and light-driven colloids [6,7]. Photo-responsive materials with dimensions of structural units at several tens of nanometers are particularly important because of the variety of new properties arising from the ensuing mesoscale structure and composition. For example, recently, researchers developed plasmonic nanostructures assembled on DNA origami templates in a powerful way that tethers the exotic optical properties of the nanoparticles to the programmability of DNA strands [9-15]. However, assembling these DNA-templated nanostructures into scalable ordered phases and mesostructured materials has proven to be challenging. Liquid crystals (LCs) have been used to assemble the nanostructures into long-range ordered composites [16-17], but conventional LCs have poor compatibility with DNA, which is very sensitive to the pH, ionic strength and organic chemical species. On the other hand, a cellulose nanofiber (CNF) colloidal dispersion, a biomaterial compatible with DNA, could be a suitable host medium capable of forming a lyotropic LC phase at a vanishing low concentration due to the large aspect ratio of CNFs. However, the utility of using such CNF-based lyotropic LCs for mesoscale colloidal organization has not be demonstrated so far.

Here we demonstrate a new composite material which comprises photo-responsive plasmonic nanomaterials templated by DNA origami colloidally dispersed in a nematic lyotropic LC. Gold nanorods (GNRs) assemble into chiral structures on DNA-origami templates, whose chirality can be reversibly switched by light. LC is readily formed by CNF at a low concentration in a nearly neutral aqueous solution. When dispersed in CNF-based lyotropic nematic LC host, the composites exhibit excellent stability and show photo-switchable chirality. Since the CNF-based LC shows very low linear birefringence, it does not significantly change the polarization of the incident light used to control the nanostructures, as well as does not alter the switchable circular dichroism of the composite. This is the first demonstration of switching between chiral and non-chiral LC medium with plasmonic optical response and circular dichroism. In more common types of chiral additives, like chiral molecules, chirality leads to helicoidal structures of director, but we achieve a completely new type of behavior, where medium is switched between chiral and non-chiral states while structure of director never becomes helicoidal but rather retains a unidirectional alignment of director [18]. This new composite may open the door for scalable fabrication of optically active material from the DNA-templated nano-scale building blocks.

GNRs with mean diameters and lengths of 20 nm × 50 nm were synthesized using seed-mediated methods in an aqueous solution

[17]. Reconfigurable chiral GNR structures were assembled using DNA origami templates, by following the procedures detailed elsewhere [10, 11]. Azobenzene molecules undergoing trans-cis photoisomerization in response to ultraviolet (UV) and visible (VIS) light were incorporated into DNA strands for reversible control of DNA hybridization and manipulation of spatial configuration of DNA origami templates. (Fig. 1a-c). DNA origami structures consisted of two 14-helix bundles with dimensions of 80 nm × 16 nm × 8 nm linked in the center by two flexible single-stranded segments (Fig. 1). The two linked origami bundles form a chiral object with a tunable angle. GNRs were attached to each origami bundle to form a chiral plasmonic nanostructure (Fig. 1c). Fig. 1c,e shows schematics and TEM images of the plasmonic dimers. The dimers exhibit binding preference to the TEM grid and the GNRs appear side by side in the TEM images (Fig. 1e).

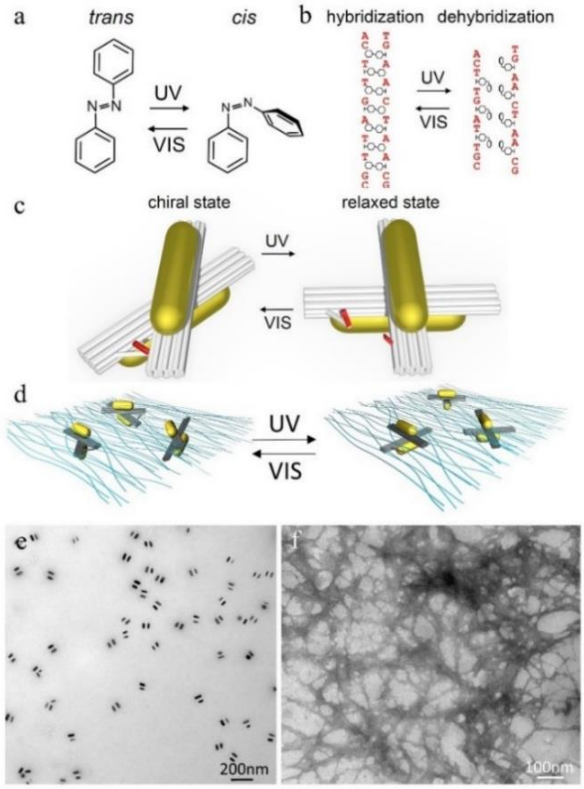


**Fig. 1.** (a) Trans–cis photoisomerization of an azobenzene molecule by ultraviolet (UV) and visible (VIS) light illumination. (b) Hybridization and dehybridization of azobenzene-modified DNA oligonucleotides controlled by trans–cis photoisomerization of azobenzene through UV and VIS light illumination. (c) Photoregulation of the gold nanorods on DNA origami template between the locked and relaxed states by UV and VIS light illumination. (d) Schematic of dispersion and photo switching of plasmonic origami in the cellulose nanofiber-based nematic LC. (e,f) TEM images of (e) DNA origami-based chiral plasmonic nanostructures and (f) negatively stained cellulose nanofibers.

To ensure an excellent dispersion of plasmonic DNA-origami in LCs, an aqueous nematic LC consisting of bio-compatible cellulose nanofibers was chosen. CNFs were produced through the oxidation of bleached wood pulp catalyzed by 2,2,6,6-tetramethylpiperidine-1-oxyl (TEMPO) radical under mild pH aqueous conditions by following the modified procedures described in literature [19]. Typically, wood pulp (1 g) was suspended in 0.05 M sodium phosphate buffer (90 mL, pH 6.8) by dissolving 16 mg of TEMPO and 1.13 g of 80% sodium chlorite in a flask. Then 455 μL of NaClO solution (13% active chlorine) was diluted ten times with the same 0.05 M buffer used as the oxidation medium and was added at one step to the flask. The flask was immediately stoppered, and the suspension was stirred at 500 rpm at 60 °C for 120 h. Then the TEMPO-oxidized cellulose fibrils were thoroughly washed with water by centrifugation at 8700 rpm for 30 min. TEMPO-pretreated cellulose fibrils were then diluted at 0.25 wt%, mechanically blended at 28,000 rpm by a food processor (Versa Pro, from Oster), homogenized by a tip sonifier (S-450, from Branson) and filtered by a membrane filter with a pore-size of 11 μm. The resulting transparent solution was then concentrated by a rotary evaporator (R-200, from Buchi) at 60 °C. The resulting CNFs are long fibers with diameters of ~4 nm and lengths of several micrometers (Fig.1f).

The plasmonic DNA-origamis were mixed with nematic CNF aqueous solution, resulting in well dispersed plasmonic composite colloids in 0.15 wt% CNF solution. Ultraviolet (365 nm) and visible (450 nm) LED lights were used to switch the configuration of plasmonic nanostructures. The photo-responsive composites were kept at a temperature of 40 °C during all switching experiments in order to ensure good switching efficiency [11].

Dark field optical imaging was performed using Olympus BX-51 microscope equipped with a 100 × oil-immersion dark-field condenser (NA=1.2), so that only highly scattered light from nanoparticles was detected. Extinction and dichroic spectra were studied using a spectrometer Cary 500 (Agilent) equipped with a linear polarizer and a quarter waveplate (400-800 nm). The extinction spectra for left-handed- and right-handed-polarized light were measured by having light pass through the linear polarizer, rotatable quarter waveplate and the sample. The circular dichroic (CD) spectra were obtained by the subtraction between the extinction of the two circularly polarized light. Transmission electron microscopy (TEM) images were obtained using a CM100 microscope (FEI Philips). Two-photon fluorescence (TPL) imaging was performed using left-and right-handed circularly polarized excitation by an 870 nm light from a tunable Ti:Sapphire oscillator (140 fs, 80 MHz, Chameleon Ultra-II, Coherent) with the setup detailed elsewhere [20].

The plasmonic nanostructures are very stable in CNF-based nematic LC host. The dispersion absorbs strongly at red wavelength due to the surface plasmon resonance from GNRs, resulting in a uniform green color of the dispersion (Fig. 2a). The electrostatic charging of the carboxylate anion on the surface of CNFs provides stabilization of the LC colloidal dispersions against aggregation in water. CNFs readily form a nematic lyotropic LC at concentrations above the critical concentration according to Onsager theory [21]. The high length-to-width aspect ratio of CNFs of approximately 500 assures the emergence of nematic LC phase behavior at the ultralow volume fractions of <0.1%, which is evidenced by the week birefringence from 1 cm-thick sample under crossed polarizers (Fig. 2b). Taking account that CNFs show weak optical anisotropy with the extraordinary and ordinary refractive indices $n_e \approx 1.59$ and $n_o \approx 1.53$ [19], the director field of the LC could be deduced from the image under cross polarizers with 530 nm-full waveplate, Fig. 2c. Because CNFs have a known positive birefringence, the blue interference color of the second order indicates the optical axis (long axis) of the CNF is parallel to the slow axis ($\gamma$) of the waveplate, while the orange interference color of the first order shows the optical axis of the CNF is perpendicular to $\gamma$ from the Michel-Levy

chart. The birefringence of the dilute colloidal dispersion of CNFs is calculated to be on the order of $10^{-5}$ based on the interference color and the length of the optical path. The good dispersion of GNRs nanostructures in CNF LC is also confirmed by the scattering from individual particle under dark-field microscope (Fig. 2d). Importantly, the composite was designed in such a way that GNRs within the origami do not experience a strong aligning potential from the LC host medium, as was the case in previous works [14-16]. Unlike in the case of individual GNRs, the dimensions of overall plasmonic DNA-origami are relatively isotropic (Fig. 2a,b), which allows them to be randomly oriented within the anisotropic host medium. This random orientation is confirmed by lack of correlated polarization dependencies of polarization-dependent scattering from nanostructures in dark field images like the ones shown in Fig. 2d. In turn, as we show below, this lack of orientational ordering of GNRs and switching of their relative orientations within the origami-based nanostructures allows us to obtain CD spectra, differently from the case of switchable linear dichroism presented in the past studies [16,17].

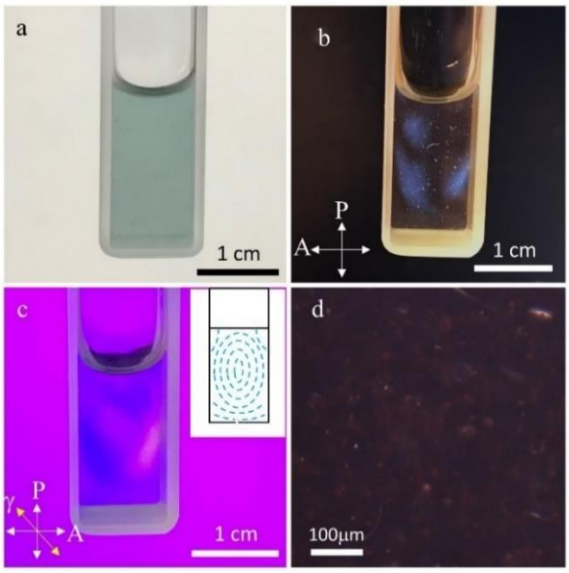


**Fig. 2.** (a) An optical photograph shows well-dispersed plasmonic DNA-origami in cellulose nanofiber solution without any aggregation or phase separation. (b,c) Weak optical birefringence of the plasmonic-LC composites is manifested under crossed polarizers (b) without and (c) with a 530 nm full waveplate. Inset in (c) schematically shows director field of the CNF-based LC. (d) Dark-field microscopy image show that the plasmonic origamis are well dispersed on the individual nanostructure basis.

The GNR assembly shows photo-switchable chirality of individual nanostructures within the nematic LC host. On visible light illumination, the azobenzene molecules are converted to trans-form and the photo-responsive DNA origami is locked into a chiral structure (Fig. 1a). When light interacts with the chiral plasmonic nanostructure, plasmons are excited in the two GNRs, leading to a characteristic extinction spectrum (Fig. 3a). Furthermore, because of the proximity of GNRs within the same DNA-origami nanostructure, the surface plasmons from the two nearby GNRs are coupled, resulting in plasmonic CD. This is revealed through characterization of CD spectra when DNA origamis are in a chiral conformation (Fig 3b). In contrast, on ultraviolet light illumination, the azobenzene molecules on DNA-origami are converted to the cis-form, resulting in dehybridization of the DNA-origami duplex (Fig. 1a). The photo-responsive segment is opened, and the conformation of the origami nanostructure is therefore relaxed into an achiral form. Consequently, the CD response after ultraviolet light illumination decreases down to vanishingly low values across the whole spectrum (Fig 3c). The plasmonic system recovers into right-handed chiral state when illuminated by blue light, again leading to the CD response across the visible wavelength (Fig. 3d). This demonstrates that visible light illumination has successfully driven the plasmonic nanostructures within the composite system into the locked chiral state. In principle, the LC medium could change the polarization state of circularly polarized light to elliptically polarized state. However, our LC system was designed in such a way that the linear birefringence of the host medium is very low. Using a 10 mm thick aligned sample and a Bereck compensator, we estimated linear birefringence to be $(1\text{-}5)\times10^{-5}$, which is consistent with low solid fraction of CNFs that themselves are weakly anisotropic and allows for neglecting the change of the polarization state of circularly polarized light as it traverses through the composite medium. Thus, our study demonstrates that DNA-origami LC composites allow for obtaining switchable CD properties. In future studies, however, linear and circular dichroism could be combined by using such nanostructures with orientational ordering within the LC and by using LCs with large linear birefringence, allowing to pre-engineer optical properties of the mesostructured plasmonic materials.

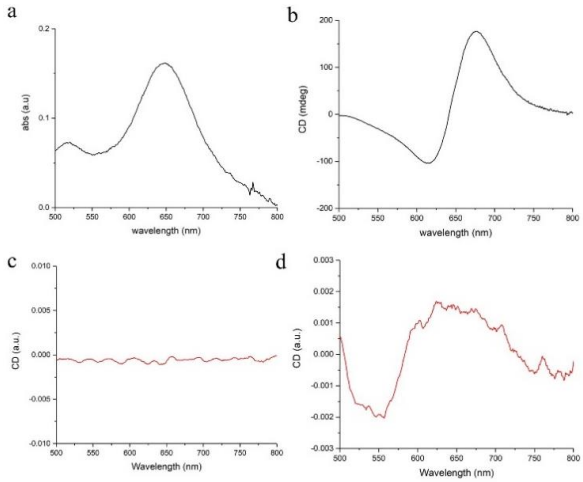


**Fig. 3.** (a) Extinction spectrum of plasmonic DNA-origami in an aqueous solution. (b) CD spectrum of plasmonic origami in aqueous solution. (c) CD spectrum of plasmonic origami in LC after UV light illumination. (d) CD spectrum of plasmonic DNA-origami in LC after blue light illumination to recover chirality of the colloidal nanostructures.

Two-photon-absorption based fluorescence signal from the GNRs excited by circularly polarized light at 870 nm confirms the good dispersion of the chiral plasmonic nanostructures in the nematic LC (Fig. 4). We did not observe the significant difference of the intensity of the fluorescence at two orthogonal polarizations. This is mainly due to the strong two-photon luminescence signal coming from the single GNR, instead of the chiral structure, where the effect of plasmonic coupling is a much weaker effect (as compared to the case of the CD). These images reveal no positional ordering of the origami nanostructures, whereas similar images for the linear polarizations of femtosecond excitation light obtained for mutually orthogonal linear polarization directions also show no

correlations between orientations of GNRs within different plasmonic nanostructures and LC director, as intended by our material design. Another interesting observation is that the chirality of plasmonic nanostructures is not transferred to macroscopic twisting of the director of the CNF-based LC host. This is likely because the dimensions of plasmonic nanostructures are much smaller than the inter-fiber distances at the used low CNF concentrations (estimated to be within 130 nm). However, future designs of LC-origami composites can involve CNFs at much higher concentrations, where switching of chiral origami nanostructures could be also accompanied by switching of LC chirality. Moreover, in addition to CNF-based nematic like host LC media, cellulose nanocrystal-based chiral colloidal LCs could be used as well.

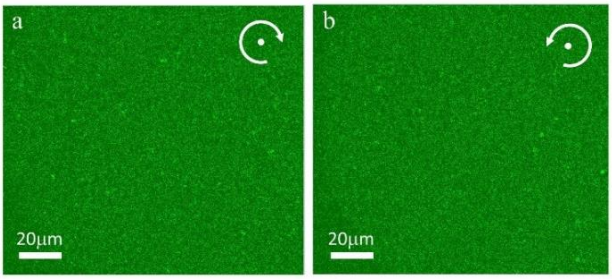


**Fig. 4.** (a)(b) Two-photon luminescence of plasmonic DNA-origami in the nematic LC under (c) right- and (d) left-handed light excitation. The luminescence is excited by 870 nm femtosecond laser light and detected within the spectral range of 400–700 nm. The left- and right-handed circular polarizations of the excitation light are marked on the images.

In conclusion, we have demonstrated the photo-switchable chirality of plasmonic DNA-origami colloidal nanostructures in a cellulose nanofiber-based nematic LC. The bio-compatible LC ensures the excellent dispersity of the plasmonic-DNA nanostructures into macroscopic mesostructured material assemblies. The low birefringence of LC host preserves the polarization of the incident light used to excite the plasmonic signal, allowing us to achieve photo-switchable circular dichroism properties of the ensuing composite. The chirality of the plasmonic assembly could be erased be UV light and recovered by visible light, resulting in photo-switchable circular dichroism. This approach may open the doors for scalable assembly of DNA origami-templated nanomaterials with multifunctionalities. The formation of mesostructured metamaterials could be potentially extended to liquid crystals formed by various types of anisotropic origami themselves [22] and is of interest for integrating with various other types of lyotropic LCs, such as chromonic LCs [23].

**Funding.** U.S. Department of Energy, Office of Basic Energy Sciences, Division of Materials Sciences and Engineering, under Awards No. ER46921 and No. DE-SC0019293. (I.I.S.). The CNF LC development component of this work was partially supported by the U.S. Department of Energy, Advanced Research Projects Agency-Energy award DE-AR0000743 (Q.L. and I.I.S.).

**Acknowledgment**. We acknowledge discussions with B. Senyuk, B. Fleury, J. De La Cruz, H. Mundoor and Y. Yuan. We acknowledge the provision of facilities and technical support by Aalto University at OtaNano-Nanomicroscopy Center (Aalto-NMC).

## References

1. Y. Zhao, and T. Ikeda eds., *Smart light-responsive materials: azobenzene-containing polymers and liquid crystals* (John Wiley & Sons.), 2009.
2. E.R. Ruskowitz, and C.A. DeForest, Nat. Rev. Mater. **3**, 17087 (2018).
3. I. Tomatsu, K. Peng, and A. Kros, Adv. Drug Deliv. Rev. **63**, 1257 (2011).
4. J.V. Hernández, E.R. Kay, and D.A. Leigh, Science, **306**, 1532 (2004).
5. R.A. Van Delden, M.K. Ter Wiel, M.M. Pollard, J. Vicario, N. Koumura, and B.L. Feringa, Nature, **437**, 1337 (2005).
6. M.E.J. Friese, T.A. Nieminen, N.R. Heckenberg, and H. Rubinsztein-Dunlop, Nature, **394**, 348 (1998).
7. M. Liu, T. Zentgraf, Y. Liu, G. Bartal, and X. Zhang, Nat. Nanotechnol. 5, 570 (2010).
8. Y. Yuan, G.N. Abuhaimed, Q. Liu, and I.I. Smalyukh, Nat. Commun. **9**, 5040 (2018).
9. A. Kuzyk, R. Schreiber, Z. Fan, G. Pardatscher, E.M. Roller, A. Högele, F. C. Simmel, A. O. Govorov, and T. Liedl, Nature, **483**, 311 (2012).
10. A. Kuzyk, R. Schreiber, H. Zhang, A.O. Govorov, T. Liedl, and N. Liu, Nat. Mater. **13**, 862 (2014).
11. A. Kuzyk, Y. Yang, X. Duan, S. Stoll, A.O. Govorov, H. Sugiyama, M. Endo, and N. Liu, Nat. Commun. **7**, 10591 (2016).
12. N. Liu, and T. Liedl, Chem Rev., 118, 3032 (2018).
13. A. Kuzyk, R. Jungmann, G.P. Acuna, and N. Liu, ACS photonics, **5**, 1151 (2018).
14. P. Wang, S. Gaitanaros, S. Lee, M. Bathe, W.M. Shih Y. Ke, J. Am. Chem. Soc. **138**, 7733 (2016).
15. J. Lee, J. H. Huh, K. Kim, S. Lee, Adv. Funct. Mater. **28**, 1707309 (2018).
16. Q. Liu, Y. Yuan, and I.I. Smalyukh, I.I., Nano Lett. **14**, 4071 (2014).
17. G.H. Sheetah, Q. Liu, and I.I. Smalyukh, Opt. Lett. **41**, 4899 (2016).
18. Y. Yuan, A. Martinez, B. Senyuk, M. Tasinkevych and I. I. Smalyukh, Nat. Mater. **17**, 71, 2018.
19. Q. Liu, and I.I. Smalyukh, Sci. Adv. **3**, e1700981 (2017).
20. Q. Liu, B. Senyuk, J. Tang, T. Lee, J. Qian, S. He, and I.I. Smalyukh, Phys. Rev. Lett. **109**, 088301 (2012).
21. P.M. Chaikin, T.C. Lubensky, and T.A. Witten, T.A., *Principles of condensed matter physics* (Cambridge University Press), 1995.
22. M. Siavashpouri, C.H. Wachauf, M. J. Zakhary, F. Praetorius, H. Dietz and Z. Dogic. Nat. Mater. **16**, 849 (2017).
23. K. Martens, T. Funck, S. Kempter, E.M. Roller, T. Liedl, B.M. Blaschke, P. Knecht, J.A. Garrido, B. Zhang, and H. Kitzerow, Small, **12**, 1658 (2016).